

## International Journal of Control Theory and Applications

ISSN : 0974-5572

© International Science Press

Volume 10 • Number 30 • 2017

### Evaluation of Local Feature Detectors and Descriptors for Look Angle Varied Terra-SAR X Band Images

**B.Sirisha<sup>a</sup> B. Sandhya<sup>a</sup> P. ChandraSekhar<sup>b</sup> and A.S. Chandrasekhara Sastry<sup>c</sup>**

<sup>a</sup>CSE Department, MVSR Engineering College Hyderabad, India

E-mail: sirishavamsi@gmail.com, sandhyab16@gmail.com

<sup>b</sup>ECE Department, Osmania University Hyderabad, India

E-mail: sekharpaidimarry@gmail.com

<sup>c</sup>ECE Department, KL University Vijayawada, India

E-mail: ascssastry@gmail.com

**Abstract:** Due to exponential growth of remote sensing sensors, the use of high resolution SAR images in diverse applications like land classification, climate monitoring, disaster management, map compiling and updating have received a remarkable boost. Such applications make use of varied image processing techniques like change detection, image fusion, 3D visualization, image alignment, which directly rely on feature extraction techniques. The success of such applications greatly depends on identifying a suitable feature detector/descriptor. Though research in the field of feature extraction, is extensive for optical images, little work has progressed for synthetic aperture radar (SAR) images whose interpretation is not always straightforward, because of the non-intuitive, side-looking geometry. The focus of this paper is to investigate and analyse the behaviour of state of art detectors and descriptors on look angle varied SAR images. We present a rigorous performance evaluation of the widely used detector and descriptor combinations on the Terra SAR X band images using objective measures like repeatability, precision and recall. The performance is evaluated using ground truth homography on a dataset comprising of all the affine transformations like rotation, scale and induced speckle noise. Through this investigation useful insights have been gained for applying state-of-the art local features to Terra SAR-X band images with diverse properties.

**Keyword:** Synthetic Aperture Radar (SAR) images, Feature detector, Feature descriptor, Repeatability.

#### 1. INTRODUCTION

Massive rise in accessibility and quality of remote sensing data and products for a wide spectrum of applications, have witnessed a steady growth over the past few years. Several remote sensing applications use Synthetic Aperture Radar (SAR) technique to acquire varied resolution images of earth surface [1]. SAR is an active sensor that transmits electromagnetic pulses and then receives the pulses that are backscattered, from the earth's surface. SAR Image is defined as a slant to ground representation of range conversion from SAR sensor. SAR image pairs acquired at different look angles contain immense amount of geometric and photometric distortion. This is due to the fact that look angle has a major influence on the backscattering pattern which results in the

objects of the same scene causing different patterns. For this reason look angle varied SAR image analysis is very demanding. The second major challenge is, due to distinct look angles, appearance of hills, bridges, tall buildings between same SAR images are considerably different. For processing of SAR images, they can either be represented by their intensity values or by extracting their characteristic features. Feature based image processing algorithms have received a boost in the recent times due to their efficiency and invariance characteristics. Quite a number of progressive algorithms have been recommended in computer vision to detect and extract the invariant characteristic features which are more suitable to optical images. An extensive category of feature detectors and descriptors prevail, the detection and description techniques and results differ based on the type of detector and descriptor used. It is evident from the survey that no particular feature extraction algorithm is suitable for all the applications, the selection of feature extraction algorithm depends on the type of image dataset used for the application. Table-I list the various feature extraction algorithms recommended for several applications and category of images [2][3]. From table-I it can be observed that

1. Most of the feature based image analysis, have focused on optical images, very little work has progressed in SAR images.
2. There has been considerable research in identifying suitable feature detector and descriptor in optical images for various image processing applications and very few papers have focused in identifying suitable detector descriptor for SAR images.

**Table 1**  
**Performance Evaluation of Image Feature Detector and Descriptor for Optical Images**

<i>S.No</i>	<i>Author-Year</i>	<i>Applications</i>	<i>Recommended Feature Extractors</i>
1.	Kaimenzeng-2016	Non-Rigid3D Objects	SIFT Detector and Descriptor
2.	Antti Hietanen-20015	Object Class Matching	Hessian Affine and SIFT descriptor
3.	Johan Johansson-2015	For Infrared Images	Hessian Affine with LIOP,ORB and BRISK
4.	Dzulfahmi, Naoya Ohta'2013	Outdoor Scene Visual Navigation	SURF Detector and Descriptor
5.	Adam Schmidt-2013	Robot Navigation	FAST Detector and BRIEF Descriptor
6.	Miksik, O., Mikolajczyk, K-2012	Optical Images	LIOP, MROGH Descriptors
7.	AL Dahl-2011	DTU Robot dataset	MSER Detector and DAISY Descriptor
8.	JL Blanco-2010	Grid Map Matching	Harris or KLT detector with circular patch descriptor
9.	Mikolajczyk, K, Schmid-2005	Optical Images-Oxford dataset	MSER detector and GLOH descriptor

Recently some researchers have worked on applying these features to SAR images. Table 2 shows list of feature extraction algorithms of computer vision used for SAR Image registration [4] [5] [6] [7] [8] [9] [10]. It is unlike the optical images as mentioned in table 1, SAR Image applications that use feature based methods mostly use SIFT and its variants for feature extraction as shown in table 2. The most widely used feature detectors; descriptors for optical images like Harris Affine, Harris Laplace, Hessian Affine, MROGH, LIOP, GLOH, sGLOH have not been analyzed.

The key objective of this paper is to exploit the benefit of invariant local features which is well utilized in optical images to Synthetic Aperture Radar images, which has been less studied. To study the behaviour of features for SAR images, a dataset consisting of all the transformations is not publicly available as in the case

of optical images. Hence we have built a dataset of SAR images using look angle varied images and applying a range of synthetic affine deformations on them. Our main contribution is evaluation of six real valued descriptors like SIFT[17], GLOH[2], sGLOH[23], Extending sGLOH(sGLOH2)[24], LIOP[25], MROGH[26] for several recently proposed scale, rotation and affine invariant detectors like SIFT [17], Harris Laplace [18], Hessian Laplace [19], Hessian Affine [20], Harris Affine [21], HarrisZ [22] using objective measures

**Table 2**  
**Feature Extraction Algorithms used in Remote sensing Applications**

S. No	SAR Image Registration		
	Type of Feature	Feature Detector/Descriptor	Author Year
1.	Corner Features	SURF + HOG	Manish I Patel'16
2.	Corner Features	SAR SIFT	F. Dellinger'15
3.	Edge Points	Pixel Migration	T.Z. Chen'14
4.	Corner points	Harris Detector	W. Zou'13
5.	Blob Features	Improved SIFT	B. Fan'13
6.	Edge Features	Bayesian	Z. Yuan'13
7.	Corner Features	Modification of SIFT	S. Suri'10

This paper is prepared as follows: Section 2 illustrate the Synthetic Aperture Radar Image formation and parameters that influence the SAR Image geometry Section 3 describes the feature detectors used in the experiments and their limitations Section 4 describes the feature descriptors used in the experiments and their limitations, Section 5 reports the experimental results and Section 6 gives the conclusion of the paper.

## 2. UNDERSTANDING SYNTHETIC APERTURE RADAR IMAGE FORMATION

SAR is a class of radar, which creates images in 3D or 2D representation of earth objects. Terra SAR X is an active sensor that transmits electromagnetic pulses and receives the pulses that are backscattered or reflected from the surface of the earth. The figure 1 shows the basic principle of SAR images .SAR instrument calculate the distance between SAR sensor and backscattered point on the surface of the earth [11]. Slant range is the calculated distance [12].The direction of the satellite is called azimuth direction and the direction normal to satellite is range direction. The angle between nadir and antenna direction is look angle. The parameters that affect the SAR Image formation are

1. Look angle of SAR sensor influence the response of backscattered. Look angle is a most vital parameter which controls the incidence angle and view geometry of the backscattered signal.
2. The second parameter is wavelength of SAR sensor, which influences the penetration depth of transmitted electromagnetic pulses.
3. As the wavelength of satellite increases, the frequency decreases. The radar bands commonly used in remote sensing and its wavelengths are Ka band 75-1.1cm, K band-1.1-1.67cm, X band 2.4-3.8 cm, C band 3.8-7.5 cm, S band 7.5-15 cm, L band 15-30 cm, P band 30-100 cm, of all these bands SAR images uses X, C, S and L band.
4. The spatial resolution influence the amount of speckle noise inject into the system. The two resolutions azimuth and range resolution influence the formation of image. Azimuth resolution is inversely proportional to antenna. Length and range resolution depends on pulse width

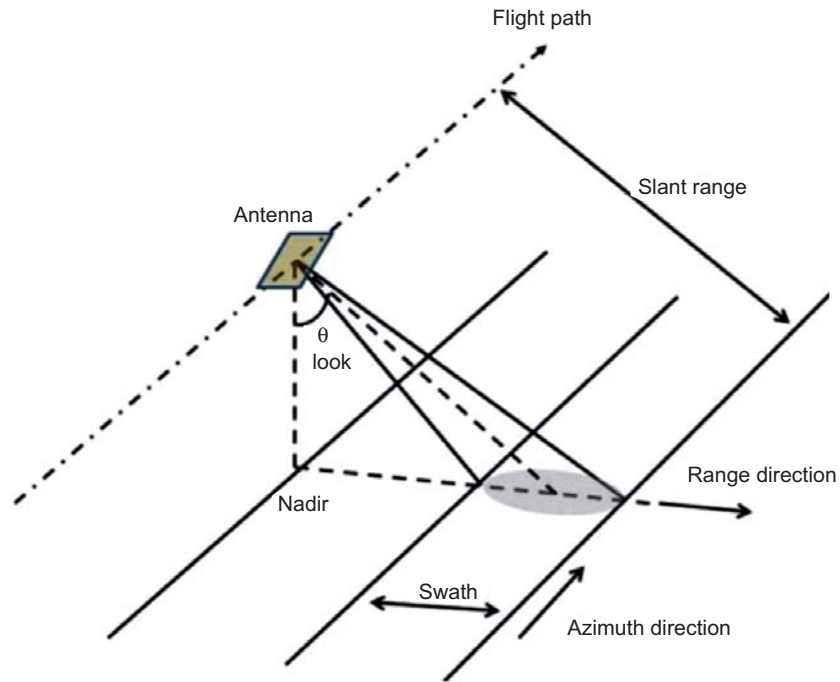


Figure 1: Synthetic Aperture Radar (SAR) Geometry

$$r_R = \frac{C\tau}{2} ;$$

$$r_A = \frac{R_{0\lambda}}{2L_0}$$

Where width and distance between target and sensor, C is pulse is fixed speed of light. The duration of pulse either high or low, there will be noise in the dataset which is very difficult to handle hence pulse compression is done using CHIRP-compressed high intensity radar pulse.

## 2.1. SAR Data Format

There are five formats of SAR Data i.e. raw data, SLC data, Multi-look data, geocoded data and polarimetric data. Raw data is original data collected from the sensor, where we cannot visualize any object *i.e.* it is simply a collection of different responses of electromagnetic signals. As we know the SAR sensor is moving and impossible to collect all the backscattered pulses at the same location. Using SAR focusing technique we will be collecting all the backscattered dispersed pulses into a single pixel of raw data. The raw data is passes through range compression, azimuth compression and yields single look complex dataset (SLC).The Doppler centroid is a vital parameter that influences the sensor look direction and affects significantly SAR image geometry.

Single look complex dataset (SLC): This is preferred dataset by the user which has complex property, where each and every resolution cell is represented by the complex number. Amplitude image is generated by square root of sum of squares of real and imaginary component.

$$\text{Amplitude Image} = \sqrt{\text{Real component}^2 + \text{Imaginary component}^2}$$

From amplitude image, intensity image is generated by

$$\text{Intensity Image} = \text{Amplitude Image}^2$$

Due to slant range distortion objects in the near range appear compressed relative to far range. Therefore there is a variation in image scale. This effect is eliminated by conversion of slant range image to grid range image. This results in rectangular pixel generation. To remove this geometric ambiguity we go for multi looking. In multi look dataset the rectangular pixels are converted into square pixels, hence user tend to move towards multi look dataset, in this dataset the ambiguity due to slant and geometry of the SAR data can be minimized. The fourth category is geo-coded dataset, which provides the user geo-referenced data i.e. we can obtain the coordinates of the objects in the scene. The fifth category is polarimetric data which provides different polarimetric combinations of the SAR Data

In this paper Terra SAR-X band dataset is used, the main features of Terra SAR X [13] are

1. Terra SAR uses active X band microwave region of the electromagnetic spectrum, which provide data of very high spatial resolution of 1 metre, 2m, 3m and 18m and the footprint for small areas is very high resolution and for large areas medium resolution. Terra SAR X operates in three main modes they are Scan SAR mode (18m), strip map mode (3m) and spotlight mode (2m) and high resolution spotlight mode (1m).
2. Active Sensor Illumination: Terra SAR uses active sensor which illuminates the surface of the earth and measure backscattered waves. Hence SAR acquires images during day as well as night.
3. Independent to state of atmosphere: The electromagnetic signals transmitted and received by Terra SAR sensor has small wavelength that can penetrate cloud and fog.
4. Unique data information: Image data generated by optical sensor comprise information of the reflective property like colour of the sensed object, where as SAR images provide information about the physical and electrical characteristics of earth surface like 1.Dielectric properties(roughness)2. Geometric structure 3.Orientation 4.Volume (moisture, oil composition).

### **3. FEATURE DETECTION**

A feature is a unique quantifiable property (characteristic) of a complete image or an object within the image and it can either be a global or local property of an image. The main characteristics of a feature include saliency, consistency, and invariance to deformations and robustness to noise. Feature detection, locates feature points or regions from image. Based on invariance property feature detectors can be classified as location invariance, scale invariance and affine invariance detector. The location invariance detector uses derivative operator (1st and 2nd order) that mainly aims to locate local extrema of a point, edge, region, maxima or minima of a curvature locations which is distinguishable from its neighbourhood. Most of the conventional detectors like Moravec's [14], Beaudet [15], Harris [16], and SUSAN etc. belong to this category. These are invariant only to rotation and not scale. In order to address scale invariance, scale space concept is used. The scale invariance detectors build a scale space and apply the operator for each scale level and finds local extrema in each region in scale space. Some of the widely used scale invariant detectors include DOG, SIFT [17] Harris Laplace [18], SURF. Affine invariance detector mainly aims to find affine shape i.e. ellipse of the local image pattern. Some of them include Harris /Hessian affine. In this section feature detectors like SIFT [17], Harris Laplace [18], Hessian Laplace [19], Hessian Affine [20], Harris Affine [21], HarrisZ [22], used in our paper are reviewed.

#### **3.1. Harris, Harris Affine and Harris Laplace Detector**

Harris is the most influential corner detector, which extended the work of Moravec [14], according to Moravec a feature point is detected by finding local maxima of minimum change in intensity .The major setback of this detector is anisotropic and fails to detect noisy edges. Harris [16] extended the work of Moravec's by

1. Presenting mathematical expansion of change of intensity for all possible shifts
2. Binary rectangular window is replaced by Gaussian smoothed circular window.
3. Regeneration of corner response as the intensity varies along the direction of shifts.

Let  $F(u, v)$  is the intensity of the pixel at position  $(u, v)$  of a gray scale image  $F$ ;  $G(x, y)$  is the weighted sum of squared difference caused by shift  $(x, y)$

$$G(x, y) = \sum_{u,v} w(u, v)(F(u + x, v + y) - F(u, v))^2$$

Where in  $w(x, y)$  = window function,  $F(u, v)$  = Intensity function,  $F(u + x, v + y)$  = shifted intensity.  $F(u + x, v + y)$  approximated by Taylors series for two dimensional function.

$$F(u + x, v + y) \approx F_x(u, v)x + F_y(u, v)y$$

$F_x, F_y$  Signify partial derivative of image  $I$  with respect to  $x, y$  by substituting this Taylor's approximation to equation

$$G(x, y) \approx \sum_{u,v} w(u, v)(F_x(u, v)x + F_y(u, v)y)^2$$

If we rewrite equation in matrix form.

$$M = \sum_{u,v} w(u, v) \begin{bmatrix} F_x^2 & F_x F_y \\ F_x F_y & F_y^2 \end{bmatrix}$$

For small shifts  $(u, v)$  the bilinear approximation

$$G(u, v) \cong (x, y)M(x, y)^2$$

For each pixel in image  $F$ , Harris matrix  $M$  is computed and then it computes Eigen values  $\lambda_1$  and  $\lambda_2$ .

1. If the Eigen value  $\lambda_1 \approx 0$  and  $\lambda_2 \approx 0$  pixel is in constant and invariable intensity
2. If the Eigen value  $\lambda_2 \gg 0$  and  $\lambda_1 \approx 0$  pixel is detected as edge.
3. If both the Eigen values  $\lambda_1, \lambda_2$  are large, pixel is detected as corner.

In order to lessen the complexity of computation

$$H = \text{Det}(M) - k(\text{Tr}(M))^2 \tag{1}$$

Threshold on corner response  $H$  and compute non max suppression. Harris corner detector is invariant and stable to rotation and translation. Since the detector detects the locations where there is large change in gradient in all directions in a pre defined scale, hence it is sensitive to image scale.

### 3.2. Harris Laplace Detector

Harris Laplace is a scale adapted Harris corner feature detector, idea is to detect corner points on various scales using Harris detector. These detected corner points are confirmed by means of Laplacian to ensure the detected scale is maxima in scale direction [18]

#### Algorithm

1. Let  $F(x)$  stand for intensity of an image. Linear scale space can be attained by convolving  $F(x)$  with Gaussian  $\sigma$

$$F(x, \sigma) = G(x, \sigma)*F(x)$$

2. Harris detector detects feature points on multiple scales, based on second moment matrix or auto correlation matrix or local shape matrix.

$$M_1(x, \gamma, \sigma) = G(x, \sigma)*(\nabla F(x, \gamma)\nabla F(x, \gamma)^T)$$

$M_1(x, \gamma, \sigma)$  Has two scale spaces with  $(\gamma, \sigma)$ ; where  $\gamma$  is derivative scale and  $\sigma$  is integration scale

- Harris corner detector detects points that have large change in orthogonal direction. Cornerness Response is  $\det(M_1(x, \gamma, \sigma)) - \alpha \text{tr}^2(M_1(x, \gamma, \sigma))$
- The scale normalized Laplacian operator

$$\Delta S = S_{xx} + S_{yy}$$

$$\Delta S(x, \sigma) = \sigma(S_{xx}(x, \sigma) + S_{yy}(x, \sigma))$$

Where  $S_{xx}$  and  $S_{yy}$  are second order partial derivatives with respect to  $x, y$ .

- Harris Laplace selects the pixel located at spatial maxima

$$x = \arg \max H_1(x, \gamma, \sigma) \quad (2)$$

- Each interest point scale is selected at local extremum over scales.

### 3.3. Harris Affine Detector

Harris Affine detector makes use of Harris Laplace to detect rotation and scale invariant corner type feature point. Harris Affine detector employ second moment matrix to determine iteratively an elliptical shaped affine region for each point [21].

#### Algorithm

- Detect set of feature points with help of multi-scale Harris measure, where scale selection is done using Laplacian operator.
- Iteratively the detected regions are refined to affine regions with help of second moment matrix.
- Affine shape is estimated using Eigen values of second moment matrix.
- Using the transformation function *i.e.*  $\sqrt{M}$  we can determine affine shape which project affine shape to one that has equal Eigen values.
- Normalize affine region to attain circular region.
- The normalized regions are linked by rotation.
- Go to step 2 if second moment matrix Eigen values are not equal.

### 3.4. Hessian, Hessian Laplace & Hessian Affine Detector

Hessian detector uses second order derivative matrix called Hessian matrix [8], which aims to detect pixel locations that comprise strong determinant values in orthogonal directions. Hessian matrix is highly responsive to ridges and blobs.

Let image  $F(x, y)$  is smoothed using a Gaussian kernel  $G(x, y, \sigma)$  to obtain  $S(x, y, \sigma)$ .

$$S(x, y, \sigma) = F(x, y) * G(x, y, \sigma)$$

The Hessian matrix of second order derivative

$$H(x, y, \sigma) = \begin{bmatrix} S_{xx}(x, y, \sigma) & S_{xy}(x, y, \sigma) \\ S_{xy}(x, y, \sigma) & S_{yy}(x, y, \sigma) \end{bmatrix}$$

The determinant of Hessian H

$$\det(H) = S_{xx}S_{yy} - S_{xy}^2 \quad (3)$$

Hessian detects blob like locations  $(x, y)$  that are invariant to rotations. Any point  $(x, y)$  if the  $\det(H)$  is local maxima to its neighbours the point is treated as feature point.

### 3.5. Hessian Laplace and Hessian Affine Detector

Hessian Laplace is a scale, translation and rotation invariant scale adapted hessian detector. Hessian Laplace detect blob like structure points on various scales using hessian detector [19]. The trace of hessian matrix is

$$tr(H) = L_{xx} + L_{yy} \quad (4)$$

Hessian Affine detector is analogous to Harris Affine detector which is affine invariant. The salient points of the image are detected using hessian Laplace detector. Once we identify the feature points, these points are refined iteratively into affine regions with help of second moment matrix. The obtained Hessian affine regions are distinguished by ellipse. [20]

### 3.6. HarrisZ Detector

Fabio Bellavia introduced Harris detector in 2011 [22]. The main idea of HarrisZ corner detector is

1. Compute a rough edge mask
2. Scale space image derivatives is enhanced by using the average gradient magnitude mask to select the pixel which is maxima on a circular neighborhood of radius  $3\sigma_D$
3. Compute a Z score function  $H_z$ .
4.  $H_z$  Corner Function =  $Z[\det(\mu)] - z[tr^2(\mu)]$
5. Select the corner points that are on the edge mask

The major pitfall is slower than other detectors.

**Implementation:** According to equation (1), as the value of  $k$  increases the sensitivity of the cornerness response function  $H$  decreases. According to Harris a point is considered to be a corner if the  $H > th_H$ , since  $th_H$  and  $K$  rely on the image structural and local properties. Z score is used for generating normalization.

$$Z(x) = \frac{x - \bar{x}}{\sigma}. \text{ where } \bar{x} \text{ and } \sigma \text{ is mean and standard deviation measure.}$$

**Step 1:** Compute the Edge mask

**Step 2:** Corner is identified by measuring cornerness strength by  $H_z$  using Z score.  $H_z$  Is the cornerness function defined over local neighbourhood obtained by integration scale  $\sigma_I$ .

$$H_z(X, \sigma_I, \sigma_D) = Z(\det(H(X, \sigma_I, \sigma_D))) - Z(\text{trace}^2(H(X, \sigma_I, \sigma_D))) \quad (5)$$

**Step 3:** If  $H_z \gg 0$  the response of corner is high compared to edge response.

$H_z \ll 0$  The edge response is high compared to corner response.

**Step 4:** According to  $H_z$ , a point is considered as a corner for which  $H_z(X) > 0$  this point attain local maxima on a circular neighborhood of radius  $3\sigma_D$  Obtained

### 3.7. SIFT Detector

#### Algorithm

**Step 1:** Scale-space extrema Detection: Detect interesting points (invariant to scale and orientation) using DOG [17].

**Step 2:** Key point Localization –Determine location and scale at each candidate location, and select them based on stability.

**Step 3:** Orientation Estimation: Use local image gradients to assigned orientation to each localized key point. Preserve theta, scale and location for each feature.



**Step 4: Orientation Assignment:** Assign constant orientation to each key point based on local image property to obtain rotational invariance. The magnitude and orientation of gradient of an image patch  $I(x, y)$  at a particular scale is:

$$m(x, y) = \sqrt{(I(x+1, y) - I(x-1, y))^2 + (I(x, y+1) - I(x, y-1))^2}$$

$$\theta(x, y) = \tan^{-1} \frac{I(x, y+1) - I(x, y-1)}{I(x+1, y) - I(x-1, y)}$$

The figure 2 shows the overview of SIFT feature detector

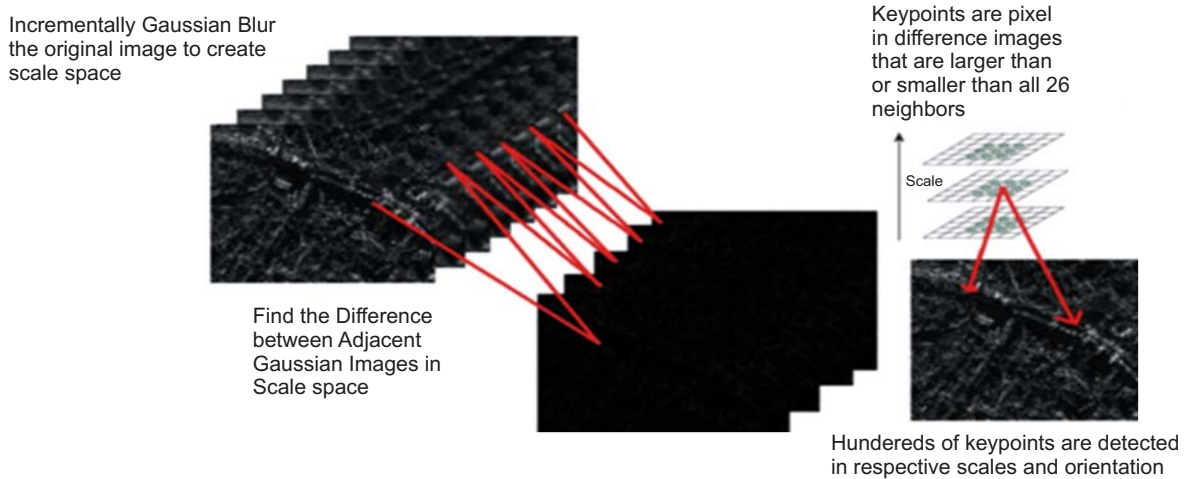


**Figure 2: The overview of SIFT Feature Detector**

## 4. FEATURE DESCRIPTION

After features have been recognized, they are extracted and described as feature descriptor or vector. A descriptor is a measurement taken from a region centered on a local point or feature defined by a feature detector. The main characteristics of feature descriptors are it can allow definite differences between the regions illumination, scale, shape, rotation and noise change. The descriptor vector extracted should be robust to background clutter and occlusion, invariant to photometric, geometric transformations. Bin Fan [27] has categorized Local Invariant Feature Descriptors as follows:

### 4.1. Based on their design methods

1. **Handcrafted:** Descriptors which use a fixed pattern of pooling regions, *i.e.* dimensionality of the descriptor is controlled by fine tuning size of the sampling grid *e.g.* SIFT and its derivatives
2. **Data-driven:** To lessen the length of descriptors researchers assimilate probability distributions for the feature point class over a quantization of the input space. In this approach feature space is quantized by thresholding over a randomly selected pixel differences

### 4.2. Based on information encoded

1. Gradient based descriptors: descriptors that are based on gradient statistics surrounded by a key point patch.
2. Intensity based descriptors: descriptors that are based on intensity statistics surrounded by a key point patch.

### 4.3. Based on data type

1. **Real Valued Descriptor:** Encodes normalized difference of orientations (*i.e.* gradients).
2. **Binary Descriptors:** Compares the intensities of sample points and the results is encoded, this makes binary descriptors faster and compact.

In this section feature descriptors like SIFT[17], GLOH[2], sGLOH[23], Extending sGLOH (sGLOH2)[24], LIOP[25], MROGH[26] are used to describe the patch around the feature point detected are reviewed.

### 4.4. SIFT Descriptor

SIFT descriptors belong to the family of histogram of oriented gradients [17]. The implementation algorithm is given

**Step 1:** Input: Image and its location are given as input to compute the descriptor vector.

**Step 2:** The input image is warped to exact location, scale, and orientation and now the features are extracted as  $16 \times 16$  pixels. The figure 3 shows the overview of SIFT feature descriptor

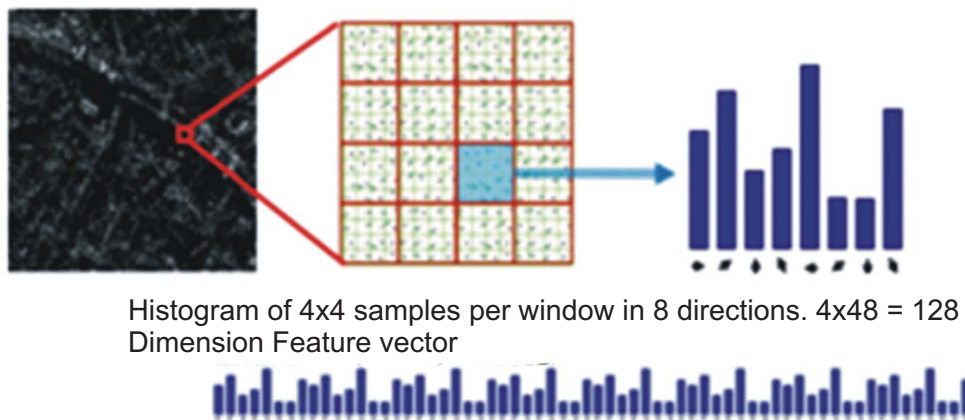


Figure 3: The overview of SIFT feature descriptors

**Step 3:** A rectangular window of  $16 \times 16$  sizes is considered in the dominant orientation direction.

**Step 4:** The region is divided into  $4 \times 4$  sub-regions. A Gaussian filter is used above the region in such a way that higher weights are given to pixel near to the center.

**Step 5:** An eight bin histogram of gradient is created for each sub-region, weighted by Gaussian window ( $\sigma$  is half the window size) and magnitude.

**Step 6:** Normalize 128 dimension descriptor vectors for illumination invariant.

### 4.5. GLOH (Gradient Local Orientation Histogram)

In SIFT the feature is divided into square grids whereas in GLOH [2] we divide into 17 log polar location grid in three various radii direction and 8 angular direction. Histogram of gradients is generated with 16 orientation bins. A feature vector of 17 location grids  $\times$  16 orientation bins is 272 dimensions. The dimensionality is reduced to 128 using principal component analysis. Figure 4 shows the overview of GLOH feature descriptors

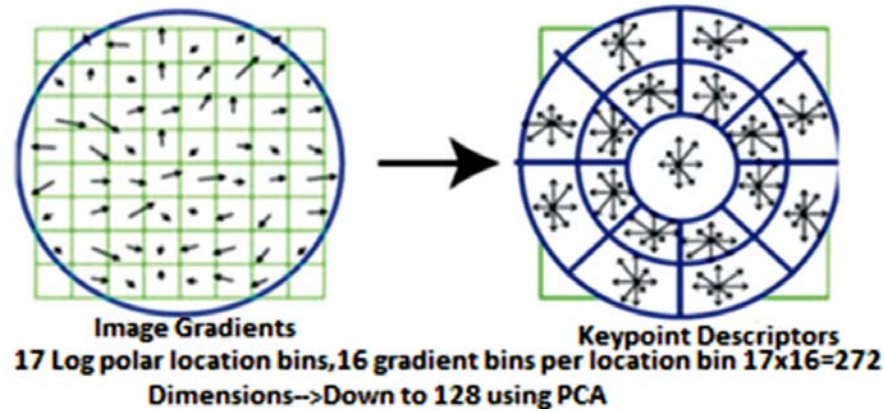


Figure 4: The overview of GLOH feature descriptors

#### 4.6. Shifting Gradient Local Orientation Histogram

In GLOH, descriptor vector is calculated using log polar grid by rotating the feature patch [23]. In Shifting GLOH (sGLOH) the feature patch is not rotated in the dominant orientation, instead the sGLOH descriptor compares discrete orientations acquired by shifting the vector descriptor. The shifted GLOH grid consists of  $n$  circular rings around the feature point. The gradient distribution, for each region is calculated by Gaussian kernel density function. Instead of rotating the feature patch we perform cyclic shift of histogram inside the circular ring. The descriptor is rotated by a  $\alpha k$  factor where  $\alpha = 2\pi / m$  this is achieved by cyclic shift of the block histogram inside a ring

$$H_{\alpha k} = \begin{cases} \bigoplus_{i=0}^n \bigoplus_{j=0}^{m-1} H_{i, [k+j]m} & \text{if } \Psi(H) = 1 \\ H_{\alpha, k} \bigoplus_{i=1}^n \bigoplus_{j=0}^{m-1} H_{i, [k+j]m} & \text{otherwise} \end{cases}$$

The distance between  $H$  and  $\bar{H}$  is

$$\widehat{D}(H, \bar{H}) = \min_{k=0, \dots, m-1} D(H, \bar{H}_{\alpha k}) \quad (7)$$

The figure5 shows the overview of sGLOH feature descriptors.

#### 4.7. Extending Shifting Gradient Local Orientation Histogram (sGLOH2)

Shifting Gradient Local Orientation Histogram descriptors performance decreases when there is a relative rotation between two sGLOH patches. In Extending Shifting Gradient Local Orientation Histogram (sGLOH2) [24], concatenate two sGLOH descriptors  $H^*$  of same patch *i.e.*  $H^1$  and  $H^2$ , where  $H^1$  is the descriptor vector obtained

by standard sGLOH and  $H^2$  is obtained after rotating the patch by  $\frac{\pi}{m}$ . The length of the descriptor is 256. The

sequence of rotation starts from 0 with each step increment to  $\frac{\pi}{m}$ . The order of rotation is  $\left\{ 0, \frac{\pi}{m}, 0, \frac{2\pi}{m}, \frac{3\pi}{m}, \dots \right\}$

the descriptors are shifted cyclically as given below

$$Q(H^*) = \{H^1_0, H^2_0, \dots, \dots, H^1_{m-1}, H^2_{m-1}\}$$

The distance between two consecutive sGLOH becomes

$$\widehat{D}_2(H^*, \widehat{H}^*) = \min_{K \in Q(\widehat{H}^*)} D(H^1_0, K) \quad (8)$$

The figure 5 shows the overview of sGLOH descriptor

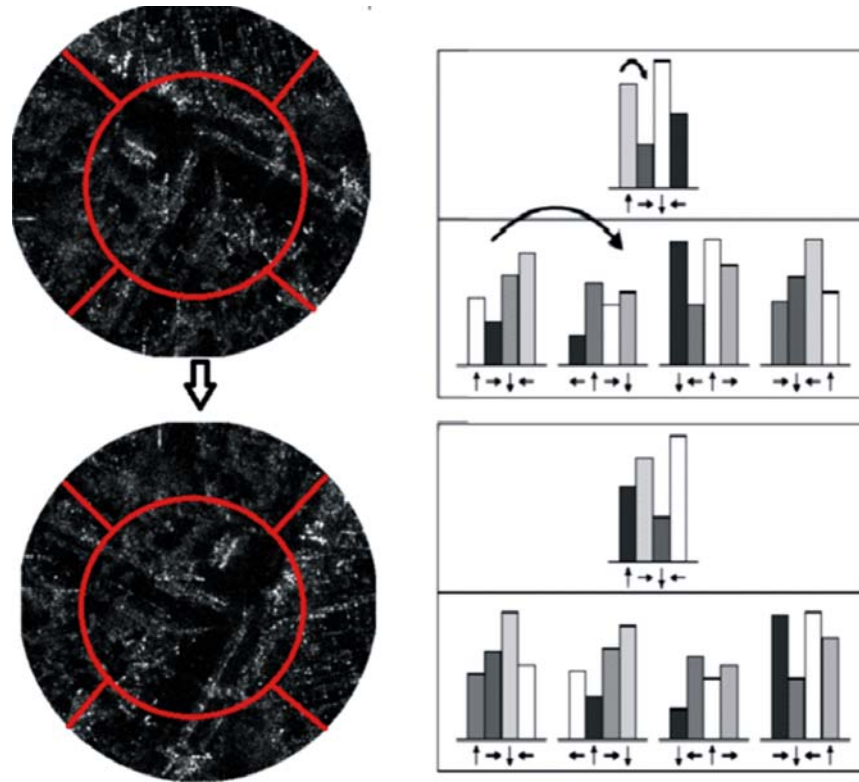


Figure 5: The overview of sGLOH feature descriptors

Multi-Support Region Order-Based Gradient Histogram Descriptor

Bin Fan et.al proposed MROGH [26] which uses features that are gradient based. Let  $P_i$  is the detected keypoint the gradient magnitude is given as  $m(P_i)$  and the orientation is  $\theta(P_i)$ .

$$m(P_i) = \sqrt{D_x(P_i^2) + D_y(P_i^2)}$$

$$\theta(P_i) = \tan^{-1} \left[ \frac{D_y(P_i)}{D_x(P_i)} \right]$$

$$D_x(P_i) = I(P_i^1) - I(P_i^5)$$

$$D_y(P_i) = I(P_i^3) - I(P_i^7)$$

Where  $P_i^j$  where  $j$  is 1,3,5,7.  $P_i^j$ 's are the keypoint neighbors in XY coordinates.  $I(P_i^j)$  is the intensity representation at  $P_i^j$ . The orientation  $\theta(P_i)$  is split into  $n$  equal bins of range  $(0, 2\pi)$

$$dis_i = \left( \frac{2\pi}{n} \right) * (i - 1) \text{ where } i = 1, 2, \dots, n$$

$$FG(X_i) = (f_1^G, f_2^G, \dots, f_d^G)$$

The gradient of  $P_i$  is given by

$$f_j^G = \begin{cases} m(P_i) \left( \frac{\frac{2\pi}{n} - \alpha(\theta(P_i), dis_j)}{2\pi} \right), & \alpha(\theta(P_i), dis_j) < \frac{2\pi}{n} \\ 0, & \text{otherwise} \end{cases}$$

Angle between  $\theta(P_i)$  and  $dis_j$  is  $\alpha(\theta(P_i), dis_j)$

$F(R_i)$  is the accumulated vector of the partition  $R_i$

$$F(R_i) = \sum_{P \in R_i} F_g(x) \quad (9)$$

#### 4.8. Local Intensity Order Pattern (LIOP)

LIOP is a handcrafted, intensity based, floating point, real valued descriptor [25]. LIOP is handcrafted because it uses a fixed pattern of pooling regions. Its dimensionality of descriptors is controlled by fine tuning the size of the sampling grid. The basic idea is

1. Smooth the image to reduce noise and then detect affine invariant regions. Normalize the detected elliptical region to a circular region.
2. According to overall intensity partition each region into several bins. Calculate LIOP point in each region.
3. Accumulate LIOP point in each bin and concatenate to create the descriptor.

##### Implementation Algorithm

**Step 1:** The local image patch is divided into sub regions using overall intensity order. These sub regions are represented as ordinal bins.

**Step 2:** The intensity order pattern of each detected feature point is obtained from the relationship among neighbor intensities of the point.

**Step 3:** For point  $x$ ,  $x_i^s$  are the keypoint neighbors in XY coordinates.  $I(x_i^s)$  is the intensity representation at  $x_i^s$ .

**Step 4:** The orientation  $\theta(x)$  is splitted into  $n$  equal bins of range  $(0, \pi)$ .

$$L(x) = I(x_1), I(x_2), \dots, I(x_N)$$

$$\gamma(L) = \pi$$

where  $\pi(I_1, I_2, I_3, \dots, I_N)$

The partition are encoded by generating index table using the index table features are mapped using mapping function  $\phi$  to map a permutation  $\pi$ .

$$\phi(\pi) = V_N^{\text{Ind}(\pi)}, \pi \in \pi^N$$

LIOP at point  $x$  is characterized as

$$LIOP(x) = \phi(\gamma(L(x)))$$

Where

$$L(x) = I(x_1), I(x_2), \dots, I(x_N)$$

The LIOP descriptors are obtained by accumulating the LIOP's of point in each sub region.

$$LIOP \text{ descriptor} = \sum_{x \in \text{bin}} LIOP(x) \quad (10)$$

### 5. EVALUATION FRAMEWORK

Cordelia Schmid [28], Mikolajczyk [3], Tuytelaars. They have introduced standard, widely accepted and established evaluation framework for assessing the performance of feature detectors and feature descriptors. In this paper we use the three major evaluation criteria for feature point detection and description *i.e.*: Repeatability, Precision and Recall. Once features from image pairs are detected and described they are matched to obtain the feature correspondence using nearest neighbor ratio.

### 5.1. Evaluation Criterion

The focus of evaluation is to check the robustness of various feature detectors and descriptors across image deformations. Feature detection is evaluated using repeatability. The detected features in addition of being stable, must be distinctive in nature. The distinctiveness is assessed by descriptors recall and precision score. The process of evaluation is described in the following steps:

**Step 1:** Let  $I_1$  and  $I_2$  be the source and target image to be matched.

$$\text{Let } P_1 = (p_1, p_2, \dots, p_n),$$

$$P_2 = (p_1, p_2, \dots, p_n)$$

are the total number of features detected from two images  $I_1$  and  $I_2$ . Let  $D_1 (P_1, R_1)$  and

$$D_2 = (P_2, R_2) \text{ be the extracted descriptors of the images } I_1 \text{ and } I_2.$$

$$\text{Repeatability} = \frac{\# \text{Correspondences}}{\text{Min}(P_1, P_2)}$$

Where,

1.  $P_1$  and  $P_2$  represent the total number of key points in Source image and target image respectively.
2. # correspondences: The total number of re-detected key points. If the distance between the matched key points of source and target images is less than some threshold then those are considered to be as the re-detected key points

The number of corresponding points is computed by finding the number of matches between key points of sensed image transformed using ground truth homography and key points of reference image. Calculate the distances between the feature descriptors  $D_1$  and  $D_2$  using vector distance measure. Find correspondence by calculating the nearest neighbor in descriptor space. Two images correspond if the vector distance between  $D_1$  and  $D_2$  below a threshold. These corresponding feature points depict the total matches between the images. In order to validate the distance measures we calculated true matches and false matches from these obtained total matches.

**Step 2:** To calculate true matches, transform the source image matched points with the estimated ground truth and calculate the distance between target images matched points and transformed points. If the resultant distance is less than 1 consider as true match otherwise false match.

$$\text{Recall} = \frac{\# \text{ True matches}}{\# \text{ Correspondences}}$$

$$1 - \text{Precision} = \frac{\# \text{ False matches}}{\# \text{ True matches} + \# \text{ False matches}}$$

### 5.2. Evaluation Dataset

Though SAR Image analysis has been studied, there exists no benchmark dataset of SAR images to compare the performance of various algorithms. Four Terra SAR X Band images of same scene in varied look angle are used for the evaluation. The specification details of Terra SAR X band images used for evaluation are

1. Acquisition Mode-Spot Light-1m resolution
2. Wavelength-Approx 3cm
3. Polarization Mode-Single

4. Polamizing Channel-VV
5. Angle of Incidence-40.9°, 41.9°, 42.9°, 43.9°[4 Images]
6. Date of Acquisition 12/oct/2008
7. Look Direction Right

The table 3 shows the dimensions of the Polarimetric SAR Data. Image1 is the source image and image 2, 3, and 4 are the target images that vary in look angle.

**Table 3**  
**Dimensions of Terra Sar X Band Images**

<i>Image</i>	<i>Dimensions</i>	<i>Deformations</i>
Img 1	9216*10556	Source Image
Img2	9216*10556	Look angle varied Image 1 (Target)
Img3	9216*10556	Look angle varied Image 2 (Target)
Img4	9216*10556	Look angle varied Image 3 (Target)

To study the behavior of features for SAR images, a dataset consisting of all the transformations is not publicly available as in the case of optical images. Hence we have built a dataset of SAR images using look angle varied images and applying a range of synthetic affine deformations like scale, rotation and induced speckle noise on them. From the standard images acquired by the Synthetic aperture radar, the dataset is generated by synthetic alteration to incorporate the desired image property. The dataset consist of 61 synthesized images. The figure 6 shows sample images used in the dataset and the deformation specifications are listed in table IV. For each pair of these images, we manually matched points and computed ground truth homography matrix which is to be used for evaluation as described in the section 5.1

**Table 4**  
**Generated Sar Dataset with Induced Deformation**

<i>Image</i>	<i>Dimensions</i>	<i>Deformations</i>
Look Angle	3 degree variation	10 Image pairs
Look Angle + Scale	Scale factor induced between source and target image is 0.5-Source scale down 0.9, Target scale up:1.8. 2-Source scale up1.8,Target scale down to 0.9. 2.5- Source scale up1.8,Target scale down to 0.7. 3- Source scale up1.8,Target scale down to 0.6 3.5- Source scale up1.8,Target scale down to 0.51. 4.5- Source scale up1.8,Target scale down to 0.4.	6 Image Pairs
Look Angle + Rotation	Angle of rotation between source and target is (10 degree to 350 degree).	35 Image Pairs
Look Angle + Speckle Noise	Induced speckle noise of variance 0.04, 0.05, 0.12, 0.16, 0.2, 0.24, 0.25, 0.32, 0.36, 0.4.	10 Image pairs

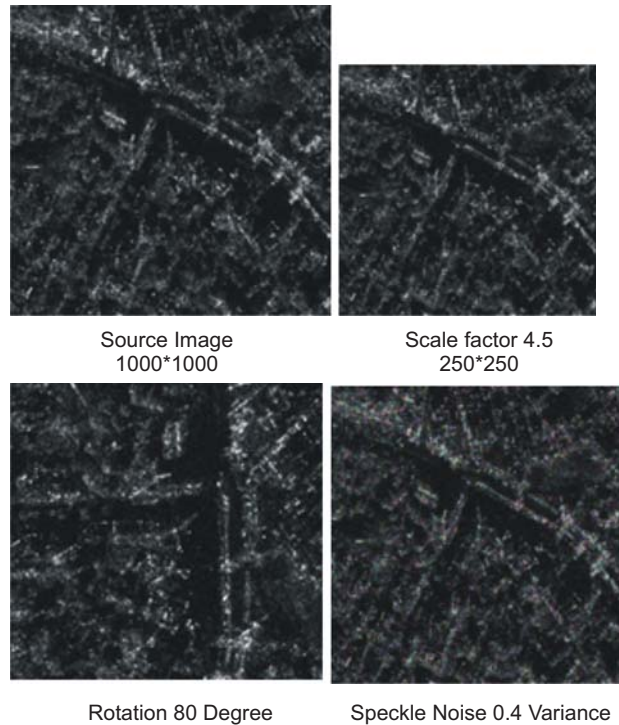


**Figure 6: Sample Dataset Images vary in Look angle + scale, Look angle + Rotation, Look angle + Speckle**

### 5.3. Implementation Details

Open CV 2.4.5 is used for implementing feature detectors and descriptors like SIFT, Hessian Affine, Harris Affine, Hessian Laplace, Harris Laplace, LIOP, MROGH, GLOH, sGLOH except sGLOH2 which is recently proposed descriptor so the binaries is used for implementation. All the salient feature points are detected and extracted with default parameters suggested by author. All the experiments are carried out on 2.19Ghz/3MB cache Intel Core™ i7,8GBRAMx64 bit, Compilation of Program code is done by MS Visual C++2010, Open CV-2.4.5

### 5.4. Evaluation Results

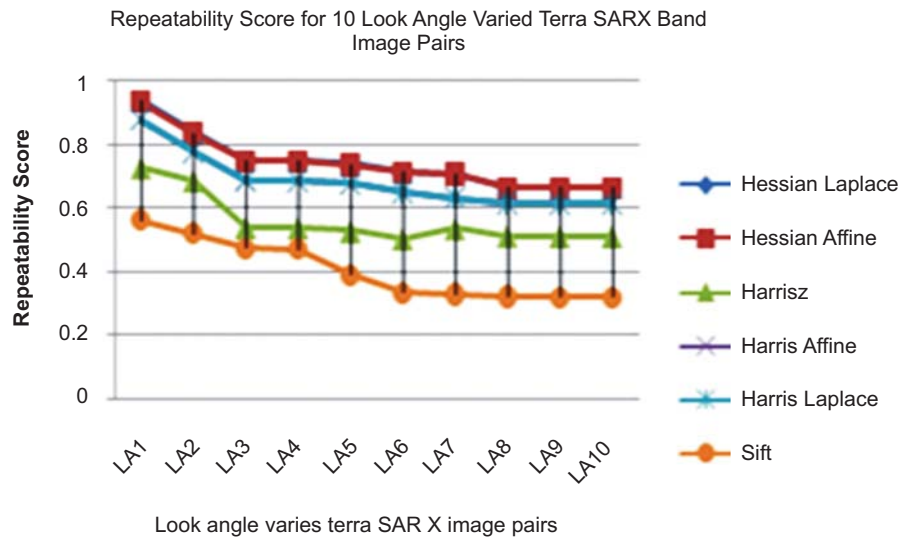
This section exhibits the results of feature detectors and descriptors used in experiments. The feature detector and descriptors used are listed in the table 5.

**Table 5**  
**Evaluated Feature Detectors and Feature Descriptors**

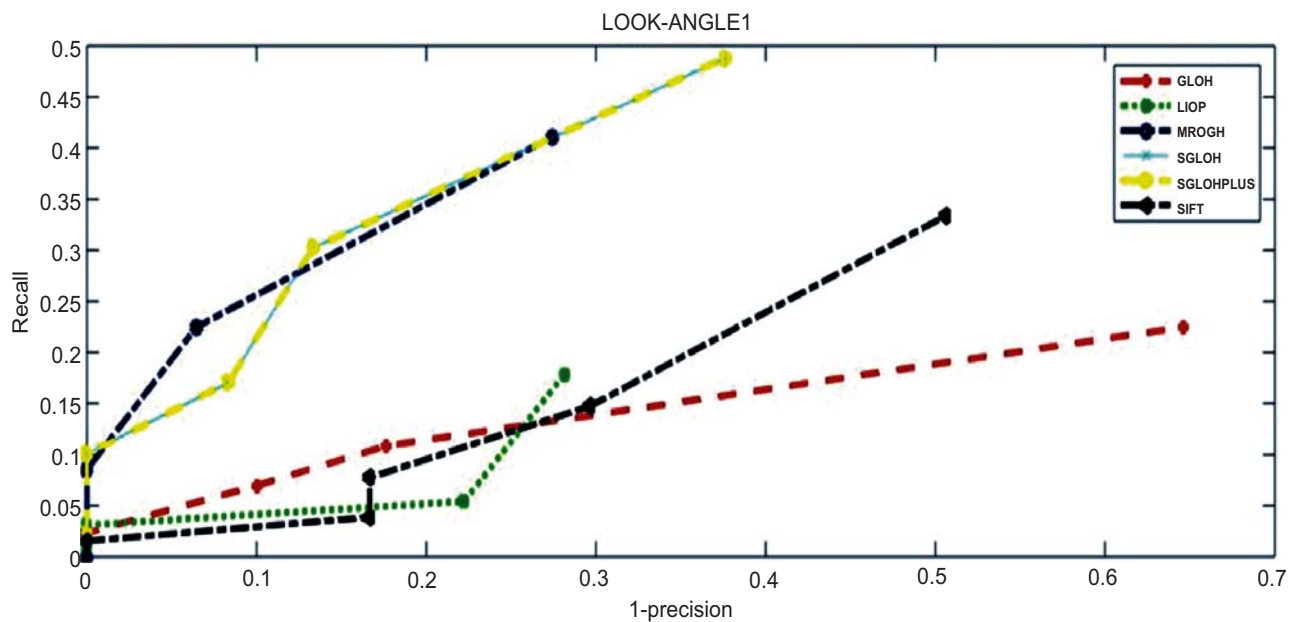
<i>Feature Detector</i>	<i>Feature Descriptor</i>
Hessian Affine	MROGH
Hessian Laplace	LIOP
Harris Affine	GLOH
Harris Laplace	SIFT
Harris Z	sGLOH
SIFT	sGLOH2



**Variation in Look Angle:** Ten pairs of look angle varied images are used in the experiment. The angle of incidence of source image is 40.9 degree and target image is 41.9 degree. Each pair of images vary in the incremental order of 1 degree .Hence Look angle difference between first pair of image is 1 degree and 10th pair of image is 10 Degree. It is observed from the figure 7(a) that the repeatability score decreases as the look angle deformation between the images increases. The repeatability score obtained using HarrisZ, SIFT, Harris Laplace detectors is smaller compared to hessian affine and hessian Laplace .Hessian based detectors selects interest point location where hessian function is maximum at any scale and also scale maxima of laplacian. Hence the determinant of hessian makes the detector viewpoint invariant.



(a)

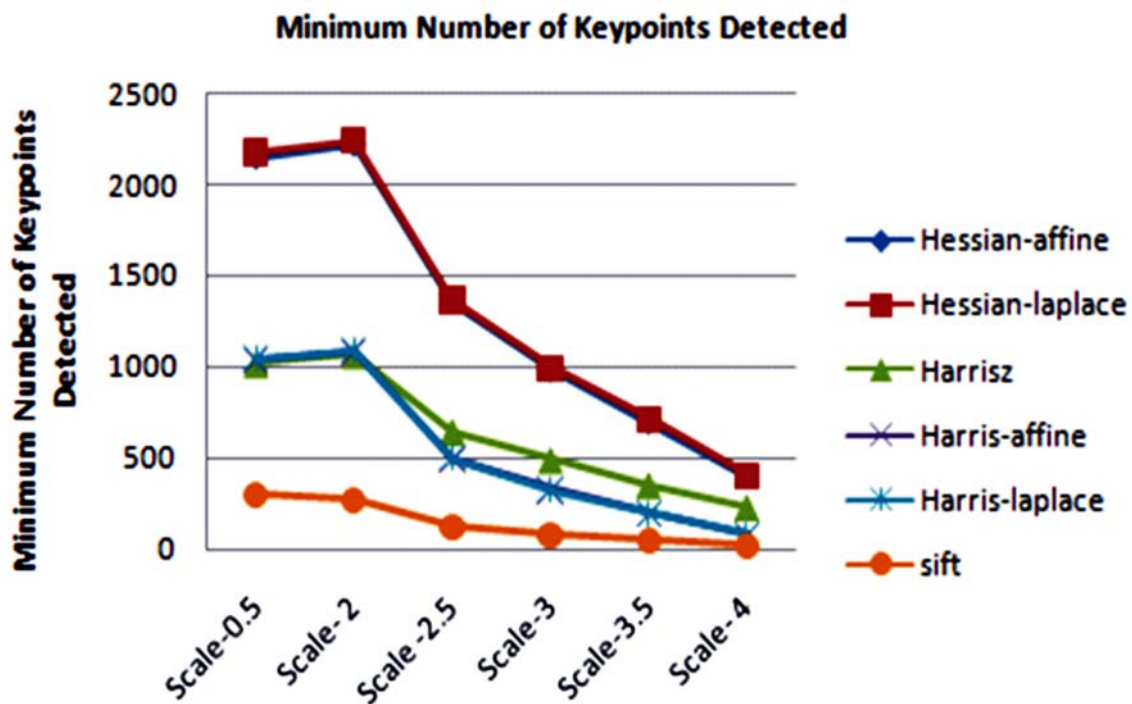


(b)

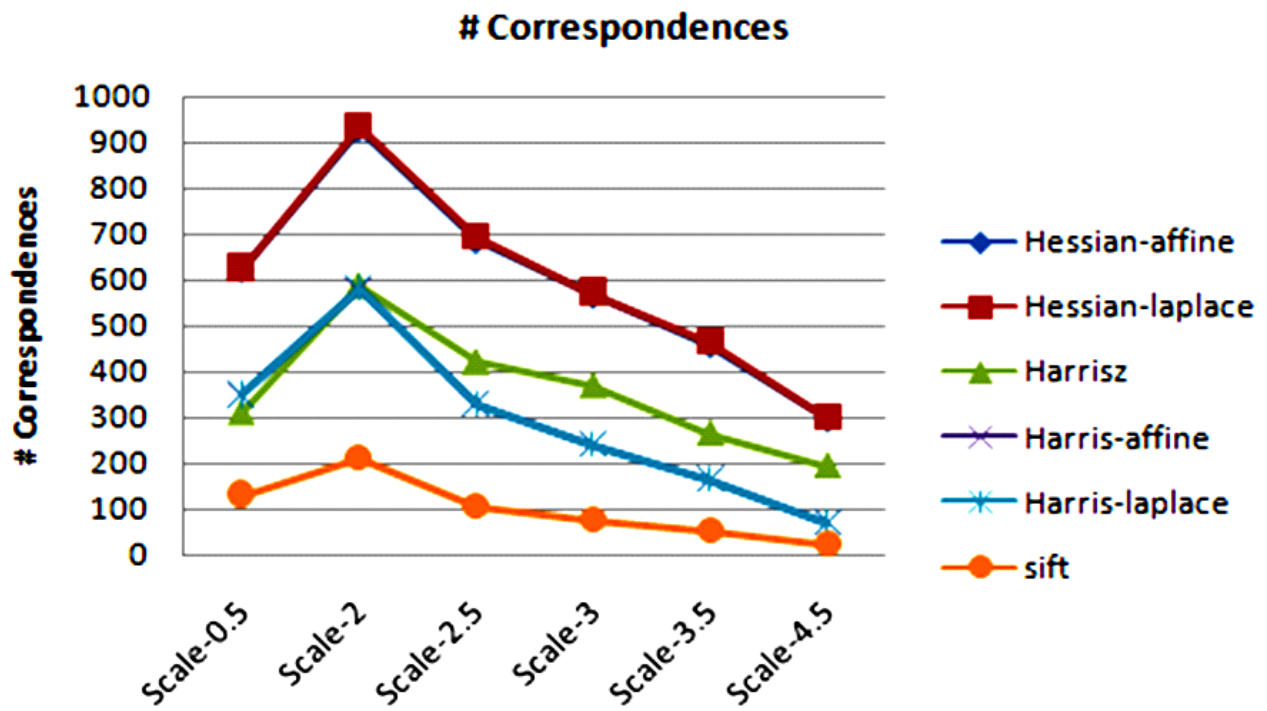
Figure 7: (a) Repeatability Score for Look Angle Varied Terra SAR X Band Image Pairs  
(b) 1-Precision Vs Recall Curve for Look Angle varied SAR images

The performance of the descriptors was evaluated using ground truth homography matrix. Nearest neighbor algorithm is used as the matching criteria *i.e.* if the distance between the matched key points of source and target image is less than threshold, they are considered as correct matches, otherwise false matches. The threshold levels considered for the experiments are 0.5, 0.6, 0.7, 0.8 and 0.9. The figure 7(b) shows 1-precision Vs Recall curve for look angle varied images. It is observed from the curve that the performance of sGLOH and Extending sGLOH2 descriptor is better than state of art descriptors like LIOP and MROGH because, sGLOH descriptor tries to incorporate several instances of descriptor of same patch at varied orientations into single feature vector by simple cyclic shift. The matching time taken for sGLOH2 is considerably high compared to sGLOH.

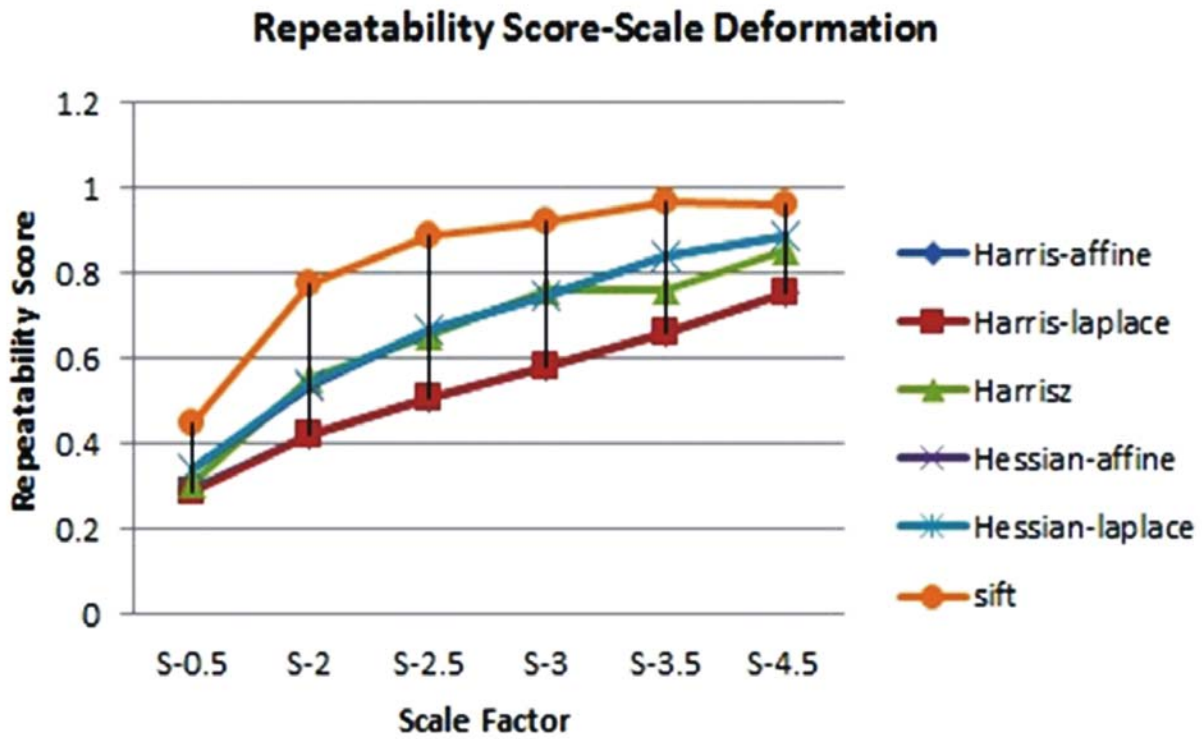
**Variation in Look Angle with Scale Deformation:** Figure 8 (a)(b) and (c) shows the Minimum number of keypoints detected, number of correspondences obtained and repeatability score for 6 look angle varied SAR images with induced scale deformation. Each pair of look angle varied images are deformed with scale factor 0.5, 2, 2.5, 3, 3.5, 4.5. From table IV it is observed that with increase in scale variation, the size of the second image with respect to first image decreased and accordingly the number of feature points detected decreases. This resulted in increase of repeatability across all detectors. However when number of correspondences are alone considered, as the scale variation increases, the number decreases. It is evident from the figure 8(b) that number of correspondence in scale 2 is high compared to scale 0.5 and 2.5. Also, Hessian Affine tends to detect more number of correspondences. This is because, the number of feature points detected by Hessian Affine is more as compared to other detectors like SIFT. The descriptor performance is seen in the figure 8 (d), which shows 1-precision Vs Recall curve. It is observed from the curve that shifting GLOH and Extending sGLOH descriptor performs better followed by MROGH. The figure 8(e) shows correspondences between source image and look angle + Scale varied Target image.



(a)



(b)



(c)

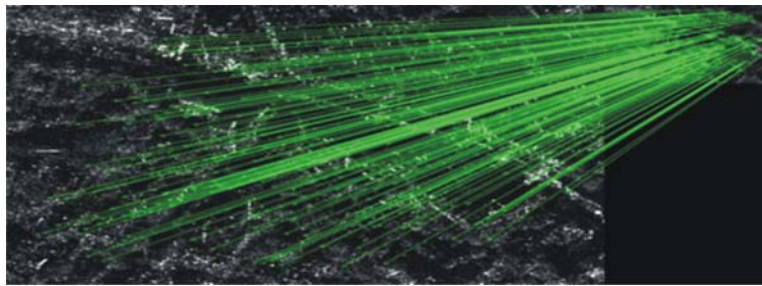
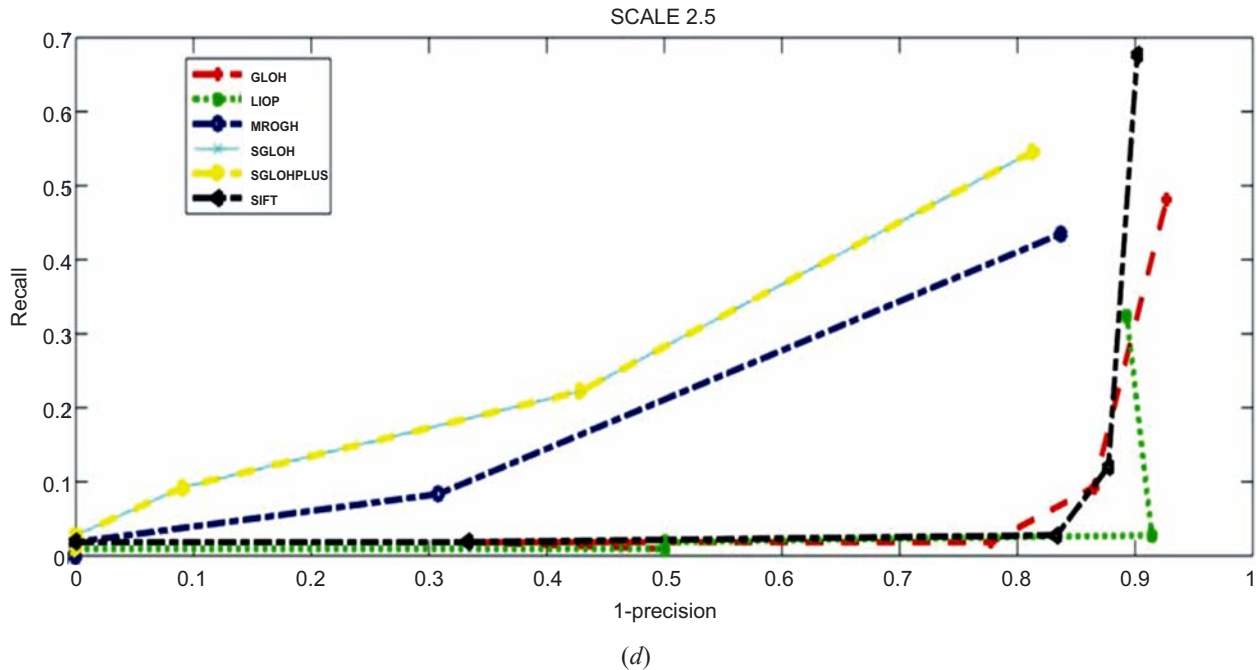
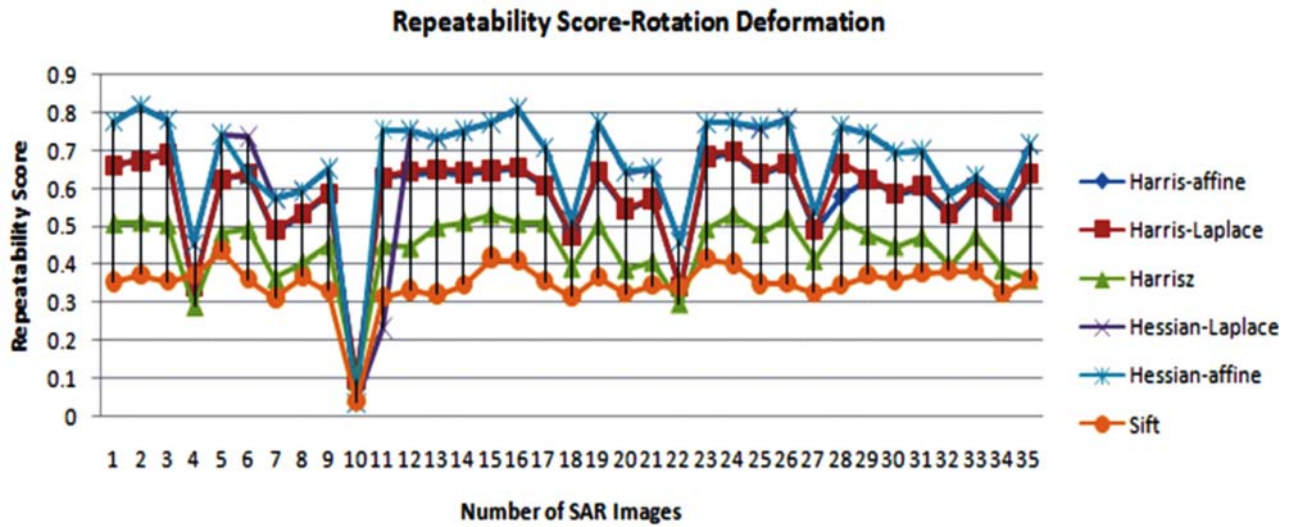
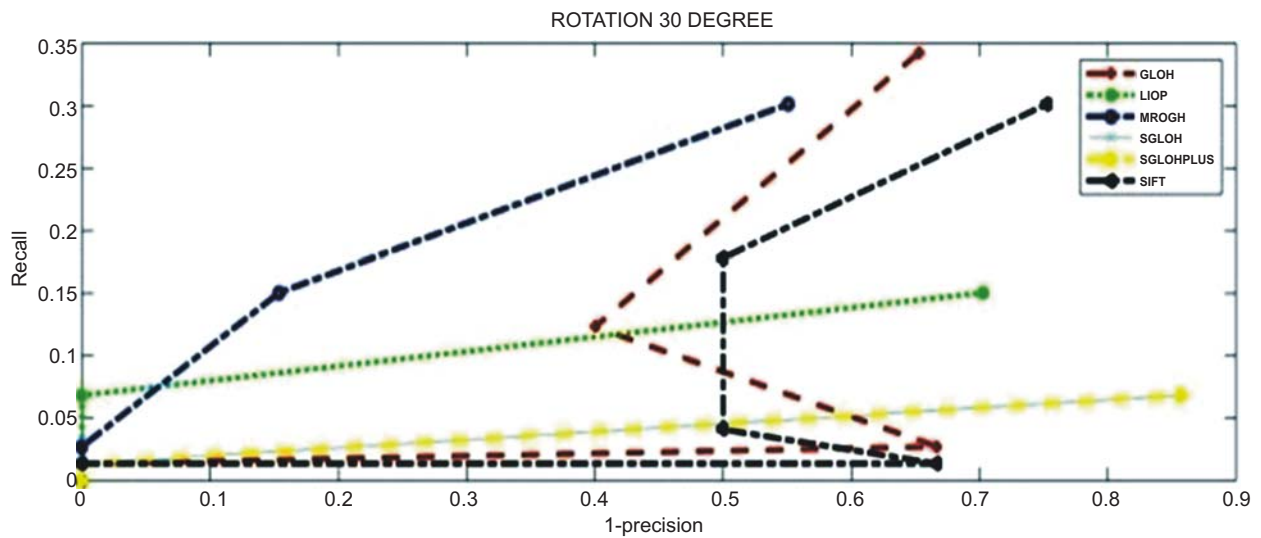


Figure 8: (a) Minimum Number of key points detected from source and target images (b) Number of Correspondences for Look Angle varied SAR images with Scale Deformation (c) Repeatability Score for Look Angle varied SAR images with Scale Deformation (d) 1-Precision Vs Recall Curve for Look Angle varied SAR images with Scale Deformation (e) Image correspondences between source image and look angle + Scale varied Target image

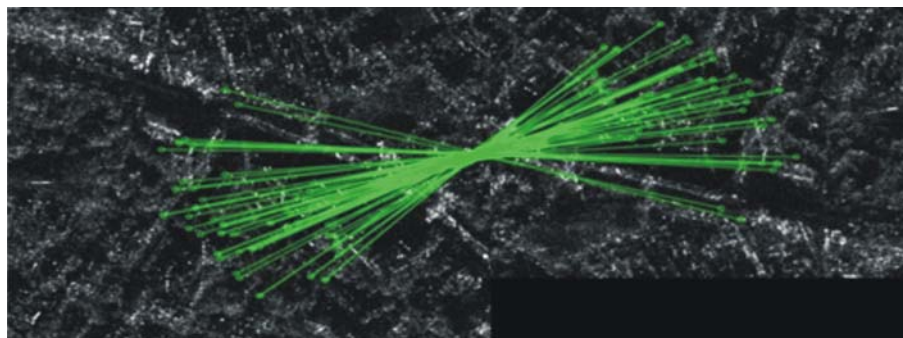
**Variation in Look Angle with Rotation Deformation:** Figure 9(a) shows the repeatability score for 35 look angle varied SAR images with induced rotation deformation. Each pair of look angle varied images are deformed with an angle of rotation ranging from 10 degree to 350 degree. In order to maintain the size of the image, the rotated target is cropped, due to this the amount of overlap between the source and target image less for certain angle(10,18,23,27,32). It is observed from the figure that repeatability score of Hessian Affine detector followed by the Hessian Laplace is consistently high irrespective to degree of rotation deformation between source and target image. Repeatability has reduced for certain angles across all the detectors, as the amount of overlap(common area) between source and target images is less for these angles which led to reduction in number of correspondences. Figure 9(b) shows 1-precision Vs Recall curve for two sample Look Angle varied SAR images with rotation deformation between image pairs are 30 degree and 60 degree. It is observed from the curve that rotation invariant descriptor like MROGH performs better than descriptors like LIOP, SIFT and sGLOH. MROGH achieves rotation invariance by pooling all the local features in multiple support regions, based on its intensity orders. The sGLOH descriptor though it is efficient and robust for look angle and scale varied images, its performance fall down when there is a relative rotation deformation between two feature point patches. The figure 9(c) shows correspondences between source image and look angle + 180° Rotated image.



(a)



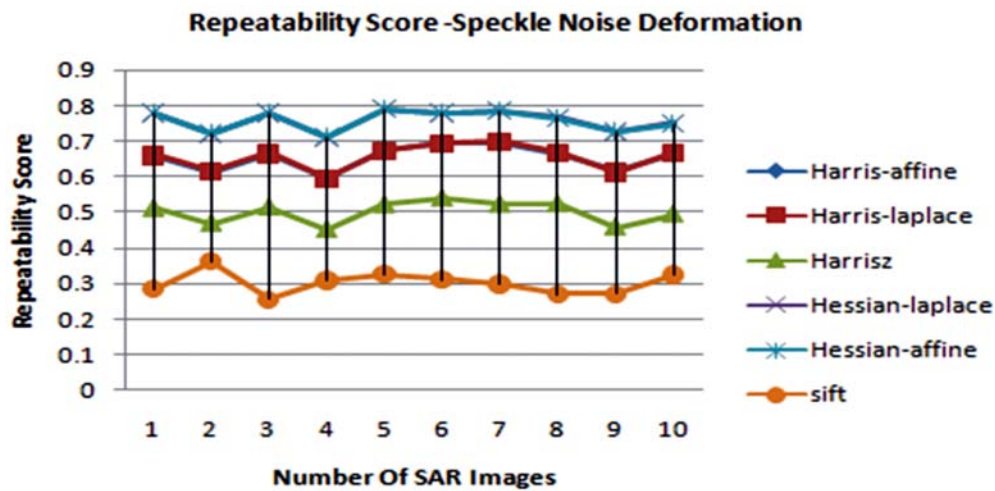
(b)



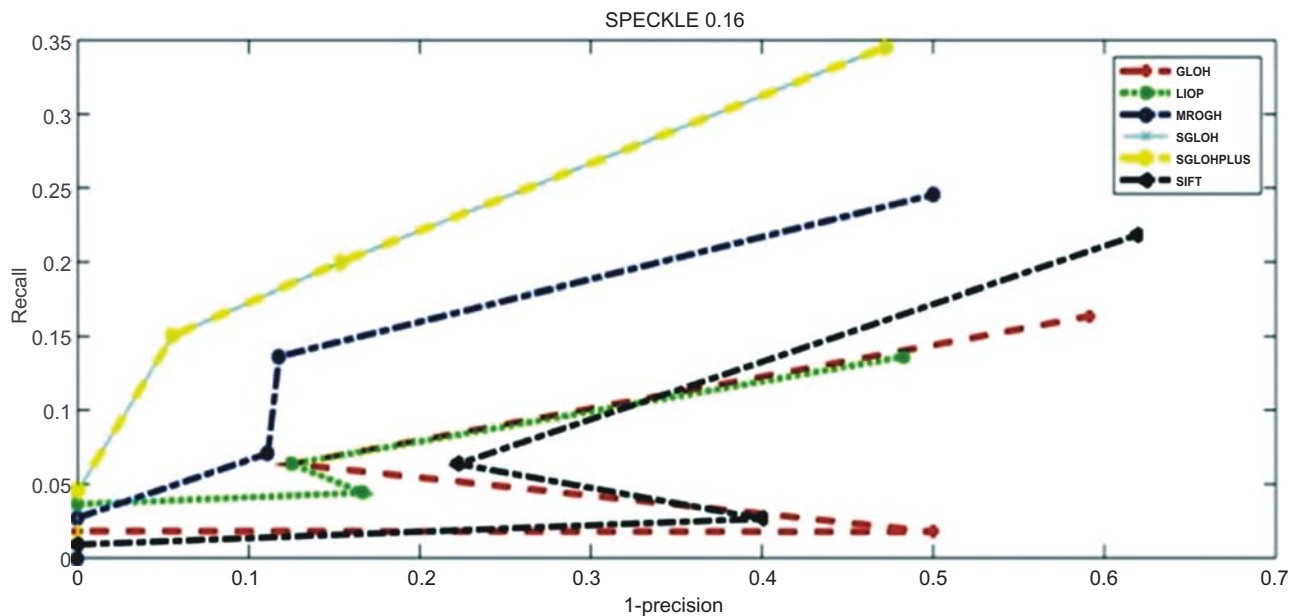
(c)

**Figure 9: (a) Repeatability Score for Look Angle varied SAR images with Rotation Deformation, (b) 1-Precision Vs Recall Curve for Look Angle + Rotation varied SAR images. (c) Correspondences between Source Image and Look Angle + 180° Rotated image**

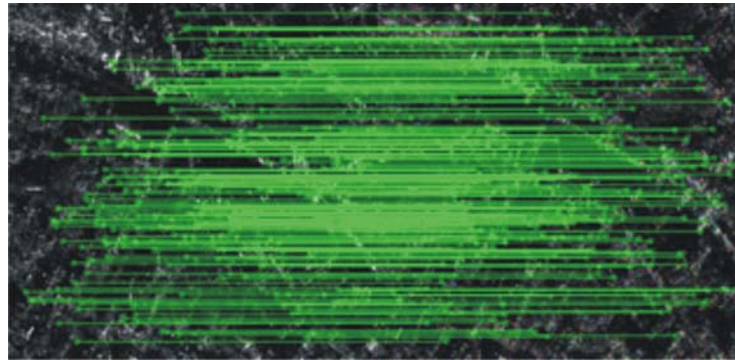
**Variation in Look Angle with Induced Speckle Noise:** Figure 10(a) shows the repeatability score for 11 look angle varied SAR images with induced speckle noise deformation. Each pair of look angle varied images is deformed with variance of 0.04, 0.05, 0.12, 0.16, 0.2, 0.24, 0.25, 0.32, 0.36, and 0.4. It is observed from the figure that as the amount of noise increases the number of correspondences decrease. Hessian Affine detector has the maximum repeatability score followed by Hessian Laplace because Hessian based detectors are more robust because the structure of blob is well localized in scale compared to corner. As observed, SIFT is sensitive to noise and performance dropped when speckle noise was added to images, this is because the local maxima of the detected point are not highly stable, since the localization is very sensitive to noise and any small variation in neighborhood texture. Figure10(b) shows 1-precision Vs Recall curve for Look Angle varied SAR images with Scale Deformation. It is observed from the curve that shifting GLOH and Extending sGLOH descriptor performs better than state of art descriptors like LIOP and MROGH. Figure 10(c) shows correspondences between source image and look angle + 0.36 Variance Speckle noise induced image.



(a)



(b)



(c)

**Figure 10: (a) Repeatability Score for Look Angle varied SAR images with Speckle Noise Deformation, (b) 1-Precision Vs Recall Curve for Look Angle +0.36 variance speckle noise induced image. (c) Correspondences between Source Image and Look Angle +0.36 Variance Speckle noise induced image**

## 6. CONCLUSIONS

In this paper we have assessed performance of widely used local feature detectors and feature descriptors on look angle varied Synthetic Aperture Radar images. Look angle variation between SAR images greatly affects the geometry and characteristics of images. We have studied the effect of look angle variation in feature detection and description for state of art detectors and descriptors. A dataset consisting of all possible geometric deformation has been built from look angle varied SAR images, and a ground truth homography matrix computed. Metrics like repeatability, precision and recall are used for evaluation. It has been observed that single detector descriptor combination cannot be efficient for all kinds of images and deformations. Classical feature detectors like SIFT, is still robust and shows good performance for scale varied SAR images. However Hessian Affine with SGLOH2 and Hessian Laplace with sGLOH descriptor have shown good performance for Look angle varied SAR Images with induced speckle noise. In addition Hessian Affine with MROGH certainly is robust in finding consistent matches across rotation deformation. As observed, SIFT is sensitive to noise and performance dropped when speckle noise was added to images. In addition, it cannot address deformations other than scale, like rotation. Hence it is efficient to use affine invariant detectors together with descriptors like sGLOH, when two SAR images have look angle and rotation based deformation.

## REFERENCES

- [1] Eineder.M.,et.al.,”Terra SAR X SAR Products and processing algorithms ”,IEEE International geosciences and remote sensing symposium,Korea,7Th july 2005:4870-4873.
- [2] Mikolajczyk, K., Schmid, C.: A performance evaluation of local descriptors. TPAMI 27(10) (2005)
- [3] Miksik, O., Mikolajczyk, K.: Evaluation of local detectors and descriptors for fast feature matching. In: ICPR. (2012)
- [4] T.Z. Chen, L.M. Chen, Y. Su”A SAR image registration method based on pixel migration of edge-point feature”
- [5] IEEE Geosci Remote Sens Lett, 11 (5) (2014), pp. 906–910
- [6] Z. Li,”Extraction of interest points by Harris interest operator for synthetic aperture radar image coregistration” IET Image Proc, 5 (2013), pp. 500–513
- [7] B. Fan, C.L. Huo ,”Registration of optical and SAR satellite images by exploring the spatial relationship of the improved SIFT”IEEE Geosci Remote Sens Lett, 10 (4) (2013), pp. 657–661
- [8] Z. Yuan, H. You, F.Q. Cai,”Bayesian edge detector for SAR imagery using discontinuity-adaptive Markov random field modeling”Chin J Aeronaut, 26 (6) (2013), pp. 1488–1497

- [9] S. Suri, P. Schwind, J. Uhl, P. Reinartz, "Modifications in the SIFT operator for effective SAR image matching", *Int. J. Image Data Fusion*, vol. 1, no. 3, pp. 243-256, Sep. 2010.
- [10] Manish I. Patel, et al, "Image Registration of Satellite Images with Varying Illumination Level Using HOG Descriptor Based SURF" Volume 93, 2016, Pages 382–388
- [11] F. Dellinger, J. Delon, Y. Gousseau, J. Michel, F. Tupin, "SAR-SIFT: A SIFT-like algorithm for SAR images", *IEEE Trans. Geosci. Remote Sens.*, vol. 53, no. 1, pp. 453-466, Jan. 2015.
- [12] J.C.Curlander and R.Mc Donough, *Synthetic Aperture Radar-System and Signal Processing* .New York:Wiley,1991
- [13] Reigber, A:et.al."Very High Resolution Airborne Synthetic Aperture Radar Imaging:Signal Processing and applications",*Proceedings of IEEE* 101(3),759-783.
- [14] R. Werninghaus, W. Balzer, St. Buckreuss, J. Mittermayer, P. Mühlbauer, "The TerraSAR-X Mission" in *EUSAR, 2004*
- [15] H.Moravec(1977) 'Towards automatic visual obstacle avoidance', in: *International Joint Conference on Artificial Intelligence,1977*, p. 584.
- [16] P.R. Beaudet(1978) 'Rotational invariant image operators', in: *IEEEInternational Conference on Pattern Recognition, 1978*, pp. 579 to 583.
- [17] C. Harris, M. Stephens(1988) 'A combined corner and edge detector', *AlveyVisionConference, 1988*,pp. 147 to 151.
- [18] Lowe, D.G.: Distinctive image features from scale-invariant keypoints. *IJCV* 60(2)(2004) 91.
- [19] K. Mikolajczyk and C. Schmid(2001) 'Indexing based on scale-invariant interest points', *Int.J. Comput. Vis* pp. 525 to531, Vancouver,Canada, 2001.
- [20] K. Mikolajczyk, C. Schmid. 2004 'Scale and affine invariant interest point detectors', *Int.J. Comput. Vis.*, 60 (2004) 63-86.
- [21] Krystian Mikolajczyk and Cordelia Schmid 'An affine invariant interest point detector', *7th Eeccv,2002*, pp128 - 142.
- [22] K. Mikolajczyk;et.al, "A comparison of affine region detectors", *Int.J. Comput. Vis* vol 65 2005;43 to 72.
- [23] F. Bellavia,et.al 'Improving Harris corner selection strategy',*IET Computer Vision.*, Issue 2, Vol.5, pp.87-96, March 2011, IET Press.
- [24] F. Bellavia,et.al"Keypoint descriptor matching with context –based orientation estimation" *.Image vision Computing* 32(9)-(559-567)-2014
- [25] F. Bellavia,et.al"Extending the sGLOH Descriptor"Image Analysis and processing *ICIAO-2015Springer-LNCS-2015*
- [26] Wang, Z., Fan, B., Wu, F, 2011' Local intensity order pattern for feature description', *IEEE International Conference on Computer Vision(2011)*603 to 610.
- [27] B. Fan, F.Wu, and Z. Hu, 2011 'Rotationally invariant descriptors using intensity order pooling ', *TPAMI* , 2011.
- [28] Bin Fan ,Zhenhua Wang, Fuchao Wu. 2013 ' Local image descriptor:MorderenApproaches ', *Springer briefs in Computer Science.*, 2016.99 Pages
- [29] Cordelia Schmid, Roger Mohr, Christian Bauckhage. Evaluation of Interest Point Detectors. *International Journal of Computer Vision, Springer Verlag, 2000*, 37 (2), pp.151.